STEPHY Publishers

Trends in Petroleum Engineering

Research Article

ISSN: 2771-2494

Evaluation of Few Layered reduced Graphene Oxide Nanocomposites in Improvement of Water based Drilling Fluids in High-Pressure High-Temperature Wells

Mustafa M Alezzi,[1] Ahmed F Ghanem,[2] Abdel Alim Hashem El Sayed,[1]* Eissa Mohamed Shokir[1]

[1]Department of Mining, Cairo University, Egypt

[2]Packaging Materials Department, National Research Centre, Egypt

Abstract

The development of thermally stable geothermal drilling mud systems is necessary for solving the possibility of drilling problems caused by HPHT conditions in geothermal wells. This occurs as a result of the degrading effects of high temperatures on mud fluids in HPHT conditions. The challenge is in designing an appropriate drilling fluid that can withstand high-pressure, high-temperature (HPHT) conditions. This study seeks to provide a new addition that is both inexpensive and eco-friendly. The additive has the potential to match or surpass the performance of existing additives when applied to HPHT drilling environments. Few-layered graphene (FLRGO) was obtained by the reduction of graphene oxide prepared according to Hummer method. Then, reduced graphene oxide surface was decorated with two types of nanoparticles in order to acquire two nanocomposites of different compositions via a simple solution mixing technique. The first graphene nanocomposite (rGB) was prepared using boron nitride (BN) nanoparticles with different ratios to yield three sets donate S from 1 to 3. The second one (rGBT) was obtained utilizing titanium nitride (TiN) nanoparticles with different percentages to yield six sets donate R from 1 to 6. The prepared reduced graphene oxide along with its nitrides nanocomposites were intensively investigated using several characterization techniques including scanning electron microscope (SEM), energy dispersive X-ray spectroscopy (EDX), Fourier transfer infrared spectroscopy (FTIR), X-ray diffraction (XRD), and thermal gravimetric analysis (TGA). At high temperatures and pressures ranging from (230°C, 17000 psi) to (80°C, 2000 psi), the study examined at how both nanocomposites affected the rheological and the filtration properties of water-based drilling fluids. Thus, 0.2, 0.6, and 1 wt. % of the optimized rGB and rGBT nanocomposites were used as additives to a mud sample and evaluated relative to the reference mud. The results emphasized that at elevated temperatures and pressures, reference sample plastic viscosity with rGBT sample containing 60% Graphene, 20 % Boron nitride and 20 % Titanium nitride was enhanced by 10 % to 59 %, 17 % to 61 % and 20 % to 67 % at (0.2 wt%), (0.6 wt.%) and (1 wt.%) concentrations respectively. Similarly, yield point was enhanced by 44% to 88%, 49 % to 88 % and 50 % to 89 % respectively. Both nanocomposites significantly decreased the filtrate loss under HPHT conditions. These findings showed that the developed nano-enhanced drilling fluids can resist the severe conditions encountered in the advanced drilling operations and possessed better thermal stability at higher temperatures.

Keywords: Nanocomposites, Water-based muds, Rheological properties, Filtration, High pressure high temperature (HPHT)

Introduction

As energy demand increases and shallow oil and gas reserves deplete, the energy industry has to discover complicated deep reservoirs which contain higher temperatures and pressures. Maintaining drilling fluid properties including rheology, filtration, and thermal stability at high temperature high pressure (HTHP) and ultra-HTHP (400-500°F and 10,000-20,000 psi) environments is challenging.[1,2] The relationship between fluid rheology, temperature, pressure, and shear history during wellbore circulation has to be examined at HPHT conditions.[3] Though water-based mud (WBM) is cost-effective and environmentally friendly, its thermal stability deteriorates at high temperatures, causing further drilling problems.[4,5] Oil-based mud (OBM) operate better in deviated wells under HPHT environments. However, OBM have drawbacks including high consumption costs and environmental

Quick Response Code:

***Corresponding author:** Abdel Alim Hashem El Sayed, Department of Mining, Petroleum and Metallurgical Engineering, Faculty of Engineering, Cairo University, Egypt

Received: 11 February, 2025 **Published:** 28 February, 2025

Citation: Mustafa M Alezzi, Ahmed F Ghanem, Abdel Alim Hashem El Sayed, Eissa Mohamed Shokir. Evaluation of Few Layered reduced Graphene Oxide Nanocomposites in Improvement of Water based Drilling Fluids in High-Pressure High-Temperature Wells: Research Article. *Trends Petro Eng.* 2025;5(1):1–20. DOI: 10.53902/TPE.2025.05.000542

impact.[6] When drilling in HT or ultra-HT formations, the fluid must have high density and endure greater temperatures, which produce many solids. Heavy solid loads create high pressures.[7] Water-created mud may break down, decreasing its viscosity and ability to limit water loss at elevated temperatures.[8] Drilling fluids must have a minimum varied rheology profile between downhole and surface properties at HPHT conditions.[9] For advanced drilling mud systems to operate in HPHT conditions and prevent mud degradation, they must have superior thermal stability.[10] Nanoparticles (NP) have better physical and chemical properties than macro and micro-sized materials. Their tiny size and high surface-to-volume ratio provide them unique mechanical, chemical, thermal, and magnetic properties. Smarter drilling fluids with specific properties that can withstand tough downhole conditions can be made using nanoparticles (NPs).[11] To improve thermal properties, Hybrid nanofluid is created by adding composite nanopowder to the basic fluid. Synergistic processes may provide hybrid nanofluid better thermal properties than base fluid and single nanoparticle nanofluid.[12,13]

Several studies have concluded that hybrid nanofluids perform stable during HPHT drilling operations. A study by Majid Sajjadian,[14] improved WBDFs using zirconium oxide, multi-walled carbon nanotubes, titanium dioxide nanohybrids, and functionalized nanotubes. Zirconium oxide improved drilling fluid rheology such plastic viscosity, yield point, and gel strength while slowly effect mud filtrate volume. Multi-walled carbon nanotubes reduce filtration without changing rheology. Hanyi Zhong,[1] used glucose-bentonite hydrothermal carbon composites (BHCCs) in WBM before and after thermal aging at 220 and 240°C. BHCCs had good filtering control by filling filter cake gaps between large particles and had no effect on bentonite dispersion rheology, unlike synthetic polymers. Xiangru Jia[15] optimized WBDFs to withstand extreme temperatures for deep and ultra-deep wells. The synthesized copolymer PAC-DDAS-SiO2 did not modify the drilling fluid's rheology. Additionally, aging at 260°C resulted in just 8 mL of filtering volume. Jalal Mohammed Zayan,[16] discusses rGO-TiO2-Ag nanocomposite and water-based nanofluids' rheology by conducting experiments at 25-50°C. Concentration, temperature, shear rate, and nanomaterials optimized viscosity and shear stress. Trinary hybrid nanofluids (THNf) enhanced viscosity by 40% for GO-TiO2-Ag and 33% for rGO-TiO2-Ag with increasing temperature and shear rate. Yuan Geng,[17] introduces triolein lubricant. Drilling fluids contained graphene and triolein after 16 hours aging at 240°C were tested. Drilling fluid lubrication was measured by friction, adhesion, and high-pressure lubricity. The drilling fluid adhesion coefficient dropped approximately 70% after adding lubricants at 240°C. The lubricant reduced friction and improved high-temperature drilling. Graphene nano plate (GNP) with triton-X100 nonionic surfactant were synthesized by Muftahu N Yahya[18] using rice husk char (RHC). GNP-RHC and GNP-TXT were compared using a water-based mud (WBM) formulation. Before and after hot rolling (AHR), all mud samples were tested for rheology, lubricity, and filtration under API and HPHT conditions. So well distributed GNP-TXT particles made GNP-TXT-based muds more stable at controlling filtration and enhancing rheological properties than GNP-RHC-based muds. However, GNP-RHC-based drilling muds controlled WBM fluid loss between 9.6 and 10.2 mL at API and 19.6 to 23.6 mL for HPHT conditions. Moreover, GNP-RHC lowered the WBM coefficient of friction of 0.45, whereas GNP-TXT decreased it more.

Lihan Rong,[19] successfully synthesized and used bi-facial grafted graphene oxide with two random and one block copolymers for water-based drilling mud at simulated downhole temperatures and pressures. Grafted graphene materials improve mud rheology at 350°F and 10,100 psi. Hanyi Zhong,[20] formulated an eco-friendly carbon coated bentonite composite (CCBC). CCBC was evaluated for fluid rheology and filtration before and after 220 and 240°C thermal aging. CCBC had minimal influence on bentonite suspension rheology, but it considerably decreased filtration loss of bentonite suspension. Taotao Luo,[21] intercalation polymerized a water-soluble monomer and lithium magnesium silicate to generate LAZ, an organic–inorganic hybrid composite. Aqueous solution yield stress increases with composite LAZ. Adding composite LAZ to 4% sodium bentonite-based slurry increased drilling fluid viscosity and dynamic shear. In drilling fluids, LAZ demonstrated exceptional temperature resistance below 150°C. Small rheological changes occur in brine drilling fluids containing composite LAZ before and after 150°C high-temperature aging. Anwar Ahmed,[22] investigated synthesizing SiO2/g-C3N4 hybrid to WBMs at various concentration to explore its effects on rheology and fluid loss. SiO2/g-C3N4 concentrations were tested before and after heat rolling (BHR and AHR). SiO2/g-C3N4 synergized with additional additives to improve rheological and fluid loss properties at higher temperatures. The results revealed increased drilling fluid thermal stability, improved yield point and 10s gel strength by 55 and 42.8% at BHR and 216 and 140% AHR. Formulation using 0.5 lb/bbl decreased fluid loss by 69.6% and 87.2% under BHR and AHR situations, respectively.

The aim of this work therefore is to develop a detailed study about the interaction of fabricated few layer reduced graphene oxide FLRGO with boron nitride BN and titanium nitride TiN nanocomposite (rGBT) in geothermal WBMs and provide an approach of enhancing the fluid loss and rheological properties under HPHT conditions. To accomplish this goal, a comprehensive experimental study with various mud samples containing rGB and rGBTs were developed and analyzed under LPLT and under high pressure and HPHT conditions to evaluate their rheology and filtration properties. r GB and r GBT were prepared in different ratios, i.e. three concentrations of few-layered graphene oxide (FLRGO) / BN and six concentrations of FLRGO/BN/TiN and tested in certain concentration (0.2 *wt.* %) of each obtained nanocomposite

in order to determine which the best nanoparticles ratio could exhibit the improved properties. Followed that, the best chosen one prepared in two extra concentrations (0.6 – 1) wt. % and evaluated. It could be claimed that, to the best of our knowledge, FLRGO or even the suggested nanocomposite has not been investigated before in WBDs according to the recent survey. However, the nanoparticles ratios were proposed by design expert software to minimize the experimental trials. The prepared samples were evaluated under low-pressure low-temperature (LPLT) and five different elevated pressures and temperatures up to (17000 psi – 230°C) as HPHT conditions. The best nanocomposite composition was characterized utilizing physical techniques such as XRD, SEM, EDX, and FTIR in order to investigate the crystal structure, morphology, elemental composition and the potential interaction.

Experimental

Materials

Bio Basic Inc. (Canada), Sd Fine-CHEM limited (India), Fisher Scientific (UK), and Carl Roth GmbH (Germany) supplied the graphite powder, potassium permanganate, sodium nitrate, and hydrogen peroxide (30%), respectively. Alpha Chemika (India) provided the titanium nitride nanoparticles (99.2%) and boron nitride nanoparticles (99.76%). Egyptian Mud Engineering and Chemicals Company (EMEC) provided chemicals such as bentonite, caustic soda, soda ash, PAC-LV and barite in order to produce blank WBM. All materials used in this study were used as they were received, without further processing.

Synthesis of few-layered reduced graphene oxide (FLRGO)

Graphene nanosheets were obtained via reduction of graphene oxide prepared by Hummer's method mentioned our previous work.[23] In the typical procedure, graphite powder was stirred in concentrated cold sulfuric acid. Then, potassium permanganate was slowly added to the mixture and the temperature was allowed to rise up to the ambient value. The mixture was left under vigorous stirring for 120 min. After that, the reaction was hydrolyzed by adding distilled water. The mixture was kept under boiling conditions. Then, hydrogen peroxide was added very slowly to the solution to avoid the effervescence. Finally, the graphite oxide suspension was sonicated for 30 minutes and then filtered out. The produced graphene oxide (GO) solid was washed several times with hot distilled water until pH~7. The resultant brown paste was then collected and dried overnight at 60°C under vacuum. To prepare graphene nanosheets, hydrazine hydrate was added to GO solution and heated in the microwave to perform the reduction process. Finally, the formed graphene flakes were separated from the solution and dried at 80°C overnight.

Synthesis of reduced graphene oxide nanocomposites

Two nanocomposites, boron nitride nanoparticles modified graphene (rGB) and boron nitride/titanium nitride modified graphene (rGBT), were prepared via solution mixing approach. Certain amount of reduced graphene oxide was dispersed in 50 mL distilled water by using sonicator for 30 min. Then, boron nitride nanoparticles of fixed weight were added to the suspended solution and the mixture was sonicated. After 30 min., the mixture was kept under vigorous stirring for 72 hours. Then, the mixture was dried to remove water at 80°C under vacuum overnight. Finally, the powder was collected and kept in the desiccator for a further using. The same previous steps were followed to modify graphene layers with both titanium nitride and boron nitride nanoparticles. Different graphene: boron nitride: titanium nitride ratios were prepared according to Table 1. The table shows the three ratios donate S from 1–3 of rGO and BN that produced the same nanocomposite with different nanomaterial percentages and the six ratios donates R from 1 to 6 between GO, BN, and TiN that resulted in the identical nanocomposite but with varying percentages of nanomaterials. Design Expert software suggested the three and the six different ratios that duplicated the previous steps.

Table 1: Concentrations variation of few-layered graphene nanocomposites

No.	Reduced Graphene Oxide %	Boron Nitride %	Titanium Nitride %
S1	20	80	0
S2	50	50	0
S3	80	20	0
R1	40	20	40
R2	40	40	20
R3	20	20	60
R4	20	60	20
R5	60	20	20
R6	20	40	40

Mud sample preparation

According to API recommended practice 13I,[24] this process involves mixing the raw materials at different percentages at a speed of 11500 rpm using a Hamilton Beach batch mixer at normal atmospheric pressure and temperature. To improve the accuracy of the study's findings, basic WBM raw materials were used. The WBM was made according to the recipe outlined in Table 2.

Techniques

Characterizations

Reduced graphene oxide and its nanocomposites were investigated using several characterization techniques. Particularly, the surface morphology was captured using the scanning electron microscope (SEM, JEOL-SEM) operating at an acceleration voltage of 80 kV. The elemental analysis was efficiently performed with energy dispersive X-ray analysis (EDX); a unit connected to SEM. The alteration in the crystallography before and after functionalization process was studied with X-ray diffraction (XRD, Bruker diffractometer, Bruker D 8 advance target). CuKα as a radiation

source and a second monochromator (λ = 1.5405) were used during the operation process. The surface functionality along with the mode of interaction within the prepared nanocomposites were illustrated using Fourier transfer infrared (FTIR, Perkin Elmer). As a crucial property in the application of water based drilling fluids, the thermal stability of the synthesized nanocomposites was inspected with Simultaneous DSC-TGA instrument (SDT Q600) under nitrogen atmosphere at a heating rate of 10°C/min starting from room temperature up to 700°C.

Table 2: Key components of WBM formulation

Product	Purity	Molecular Weight (g/mol)	Density (kg/m3)	Concentration (ppb)	Mixing Time (min)	Function of materials
Tap Water	99.96%	18.015	1000	320	-	Base liquid
Pre-hydrated bentonite	80 - 90 %	180.1	1100	22.5	15	Viscosifier
Caustic Soda	99%	39.997	2130	0.1	5	pH enhancer
Soda Ash	99.70%	105.988	1200	0.1	5	Softness of water
Polyanionic Cellulose (PAC – LV)	98%	1.146	2.85	1	5	Filtrate loss reducer
Barite	98%	233.4	4500	75	20	Weighting material

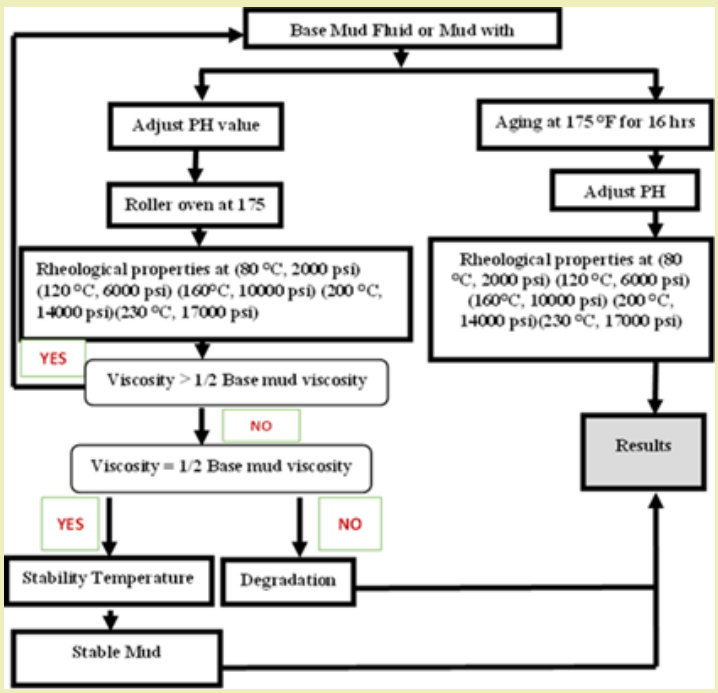

Figure 1: Flowchart with the steps taken in this study to evaluate the designed muds

Water based drilling fluid evaluation

Drilling fluid components were mixed and sheared with the produced nano composites using a Hamilton Beach mixer. Using a hot roller oven, samples of produced drilling fluid were exposed to a temperature of 80 °C. It is noteworthy that (0.2 wt.%) of each nanocomposites of rGB and rGBT obtained in tables 1 and 2 was added to the prepared mud in order to investigate the associated properties in HPHT conditions. Consequently, eleven mud compositions were prepared and examined in comparison to the blank composition. The optimum chosen sample of rGB compared with the optimum one from rGBT list to examine the effectiveness of titanium nitride NP addition. Finally, the best sample tested and evaluated in 0.6 and 1 wt. % for its rheological and filtration properties as it is already tested at 0.2 wt. % in the previous work.

Under low-pressure low-temperature conditions, the shear stress and the shear rate of the drilling fluid were measured by the viscometer (6-speed VG meter) to calculate the plastic viscosity (Pv) and yield point (Yp) according to 13I-API standard procedure.[24] Additionally, the following equations were used to determine the rheological properties of drilling mud, such as AV (Eq. 1), PV (Eq. 2), and YP (Eq. 3):

$$AV = \theta600/2 \quad (1)$$

$$PV = \theta600 - \theta300 \quad (2)$$

$$YP = \theta300 - PV \quad (3)$$

Where, θ600 = Dial reading at 600 RPM and θ300 = Dial reading at 300 RPM.

Concerning the high-pressure high-temperature rheology test, Model 77 HPHT viscometer was used to calculate PV, YP and gel strength for all samples. The HTHP Viscometer linked with the user-friendly ORCADA® software. The applied pressure and temperatures were as follow: ((2000 psi-80°C), (6000 psi-120°C), (10000 psi-160°C), (14000 psi-200°C) and (17000 psi-230°C)). Figure 1 displays a flow diagram with the staged carried out in this experimental research to analyze the designed samples.

Furthermore, the HPHT filter press records the fluid loss volume (filtration) as double number of millimeters lost, with a differential pressure of 500 psi and a temperature of 250°F. The mud cake thickness created on filter paper was gauged at the end of the experiment.

Results and Discussions

The experimental results were categorized into two primary parts.

The initial section provides data on the apparent viscosity (AV), plastic viscosity (PV), yield point (YP), and gel strength (Gel10s, Gel10 min) of a water-based fluid (WBF) when (rGB) and (rGBT) nanocomposites were added at (80 °C, 14.7 psi) as LPLT condition. The next part examines the study of the WBM rheological and filtration properties, which is enhanced by (rGB) and (rGBT) nanocomposites under HPHT conditions. The density of all the samples remained constant at 10 ± 0.1 (ppg) throughout the investigation.

Characterization of graphene nanocomposites

X-ray Diffraction (XRD)

XRD was used as a powerful technique to investigate the crystallography of the obtained nanocomposites. As depicted in Figure 2A, reduced graphene oxide has a broad peak at ~ 25° confirming successful exfoliation of graphite oxide into few-layered graphene during the reduction process in agreement with published articles.[25] In order to discuss the modification process, XRD was performed for commercial nanoparticles. Particularly, boron nitride nanoparticles showed characteristic lines at 12.7°, 26.7°, 41.6°, 55.1°, and 75.7° corresponding to [001], [002], [100], [004], and [110] reflection planes in accordance with state of art,[26,27] Figure 2B. Meanwhile, titanium nitride spectrum showed other peaks at 36.5°, 42.5°, 61.7°, and 73.9° assigned to [111], [200], [220], and [311] reflection planes,[28,29] Figure 2C. However, modification of nano graphene with the nanoparticles caused a significant broadening in the peak at 12.7° with a slight shift in the other main peaks of boron nitride and titanium nitride, Figure 2C-D. This might be attributed to a strong physical interaction was established between graphene surface and the guest nanoparticles.

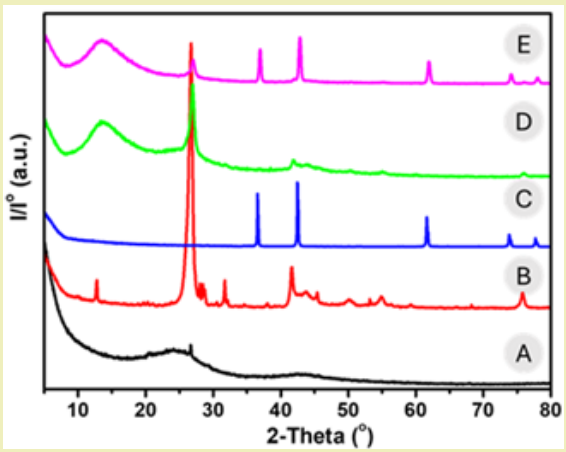

Figure 2: XRD spectra for [A] Few-layered graphene nanosheets, [B] Commercial boron nitride nanoparticles, [C] Commercial titanium nitride, [D] Boron nitride modified graphene, and [E] Boron nitride / titanium nitride modified graphene

Scanning electron microscope (SEM)

Images of scanning electron microscope provide more information about the surface morphology of graphene nanolayers before and after modification with the nanoparticles. Figure 3A shows the fluffy layers of graphene which deem the distinguished morphology of nanostructure graphene. Boron nitride and titanium nitride nanoparticles were significantly decorated the surface of graphene layers (red and green arrows), Figure 3B-C, which confirmed the feasibility of solution mixing approach used for preparation. However, some nanoparticles aggregates can be observed (blue arrows), Figure 3C. On the other hand, the micrographs of mud before and after addition of GBT nanocomposite mostly did not show a significant change which emphasized the good dispersion of the nanocomposite and its fusion with the mud' components, Figure 3D-E.

Energy Dispersive X-ray Spectroscopy (EDX)

EDX was performed in order to confirm the presence of nanoparticles on the surface of graphene. Figure 4A shows the spectrum of firstly prepared nanocomposite based on boron nitride only. Obviously, the characteristic bands of BN were located at their

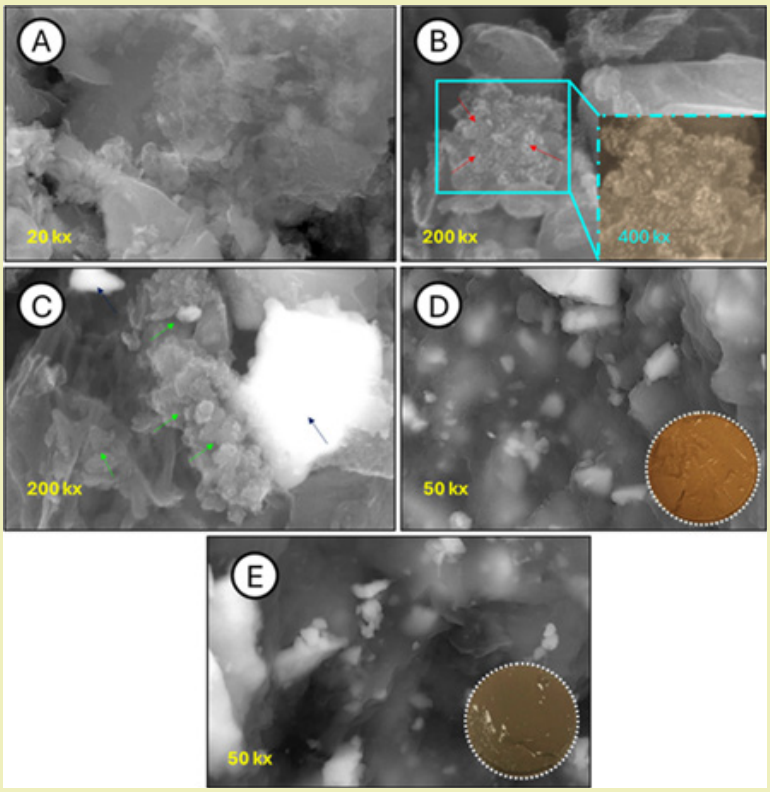

Figure 3: SEM micrographs for [A] Few-layered graphene nanosheets, [B] boron nitride nanoparticles modified graphene, [C] Boron nitride / titanium nitride modified graphene, [D] Blank mud, and [E] Graphene/ boron nitride / titanium nitride modified mud. The insets are the digital pictures for the filter cake for the optimized mud samples

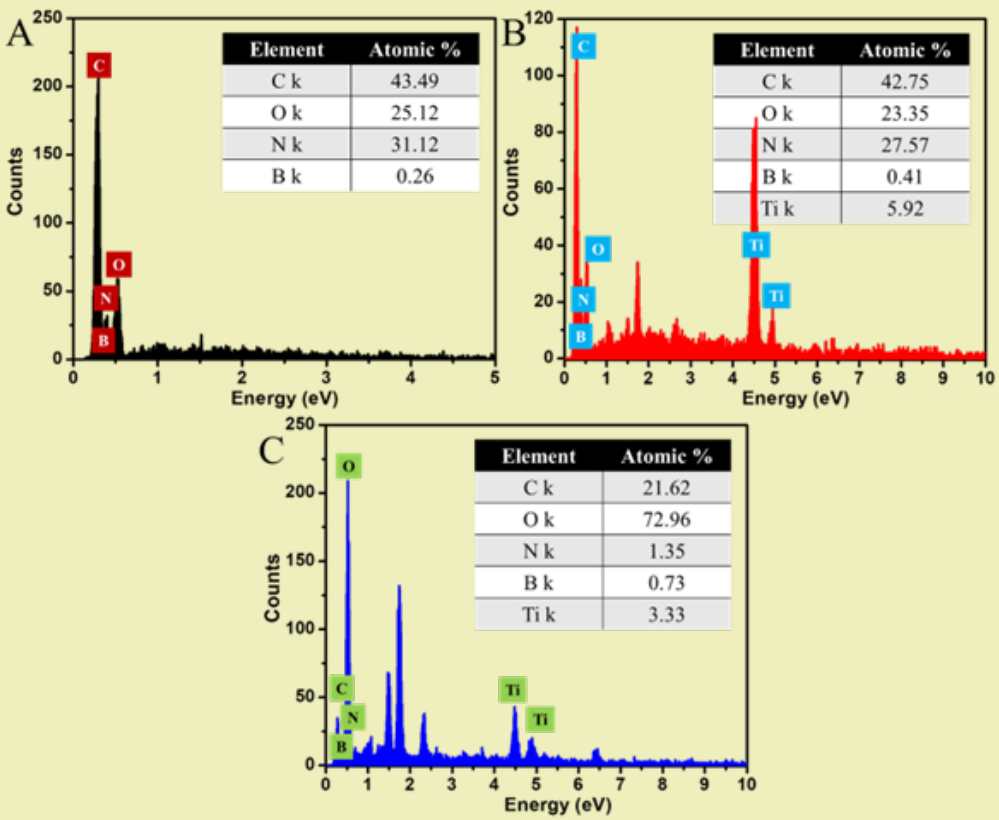

Figure 4: EDX spectra for [A] Boron nitride modified graphene, [B] Boron nitride / titanium nitride modified graphene, and [C] Graphene/ boron nitride / titanium nitride modified mud

Indeed, the oxygen atoms were appeared in the prepared graphene nanocomposites which might be attributed to the incomplete reduction of graphene oxide into its reduced form. Ghanem et.al. and others reported that it is difficult to reduce all the oxygenated functional groups on the graphene surface.[25,32-35] Similarly, EDX of GBT sample exhibited the distinctive lines of titanium nitride[35] accompanied with the boron nitride ones, Figure 4B, confirming the successful surface decoration with both nitrides nanoparticles. Despite SEM could not distinguish the modified graphene layers in the modified mud sample, EDX confirmed the presence of nanocomposite. Figure 4C depicts the spectrum of modified mud. As shown, the characteristic bands of carbon, boron, titanium, and nitrogen are pronounced in their position which proved the successful inclusion of the nanocomposite with the mud matrix. This sample displayed superior properties in the target application as will be discussed later on. It is worth to mention that, the increasing of oxygen peak intensity particularly in this sample might be revealed to the mud components. The inset tables present the atomic percentage of each element in the sample under investigation.

Fourier transfer infrared (FTIR)

Fourier transfer infrared technique was used to investigate the nature of interaction between graphene surface and the nanoparticles, Figure 5. Particularly, the prepared graphene nanosheets showed mostly free oxygen bands spectrum, Figure 5A, as a result of reduction process.[36] Boron nitride displayed main bands at ~ 3400, ~ 1410, and ~ 790 cm^{-1} attributed to B-OH, B-N-B, and B-N stretching, respectively. Mostafa[37] has recorded the same results while modification of graphene oxide with boron nitride nanoparticles. Figure 5C demonstrates the characteristic bands of titanium nitride that pronounced at ~ 3400 and ~ 685 cm^{-1} assigned to Ti-OH and Ti-N, respectively.[38] The spectra of prepared nanocomposites showed a combination off the previous bands with a significant shift which confirmed the strong interaction between graphene sheets and the nitride nanoparticles, Figure 5D-E.

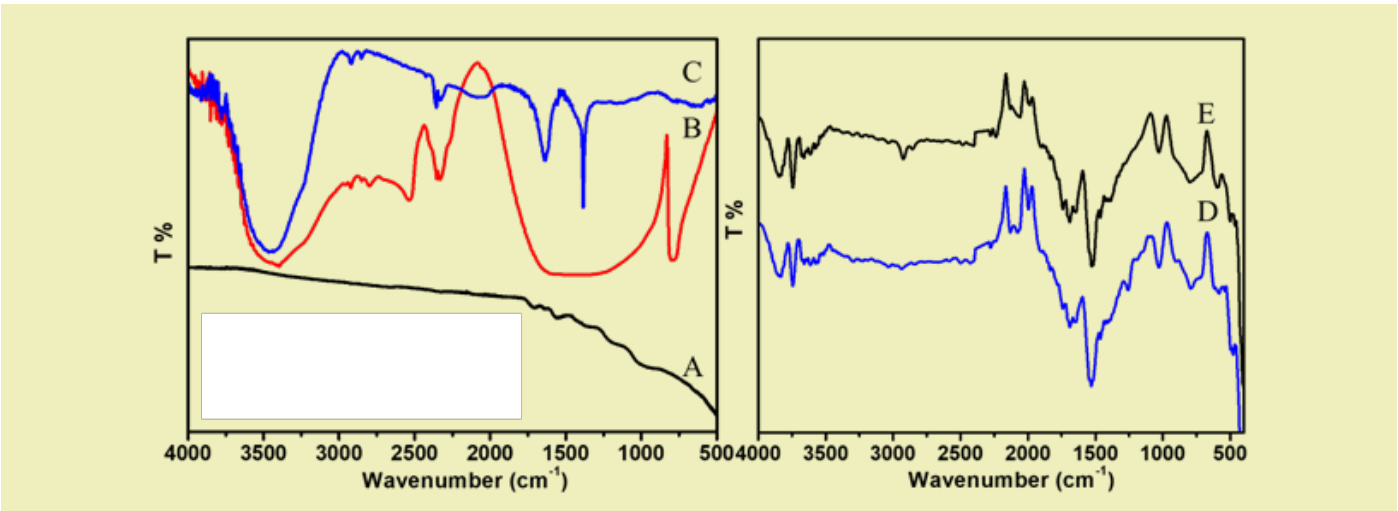

Figure 5: FTIR spectra for [A] Few-layered graphene nanosheets, [B]Commercial boron nitride nanoparticles, [C] Commercial titanium nitride, [D] Boron nitride modified graphene, and [E] Boron nitride / titanium nitride modified graphene

Thermal gravimetric analysis (TGA)

Thermal analysis was also investigated, despite the working temperature in this study was up to 230°C i.e. the thermal stability of graphene and nanoparticles is high according to the previous studies[39-41] and definitely exceeded the working temperature reached in the experimental part. However, TGA thermograms confirmed much thermal stability of GBT than GB nanocomposite thanks to the introduction of TiN particles. As depicted in Figure 6 [Top], both nanocomposites showed two steps; the first step started ~ 70°C and ended ~ 100°C due to removal of solvent molecules. The second step was started at ~ 410°C for GB sample, meanwhile GBT started degradation at ~ 440 °C confirming increment in the thermal stability. Particularly, most of sample weight was lost in the second step. Moreover, DTA confirmed a slight shift in the degradation temperature of both nanocomposites, Figure 6 [Bottom]. It could be claimed that, both prepared graphene nanocomposites are thermally stable in the temperature up to 400°C which considers a further prove for their high workability in HTHP drilling fluid applications.

Rheological and flow behavior properties

Effect of rGB/rGBT nanocomposites on rheological properties and flow behavior of WBM at HPHT condition

- *Effect of rGB nanocomposite components ratios on the rheological properties of WBM*

Conventional additives in drilling fluid may degrade thermally at high temperatures, affecting rheological and filtration properties such plastic viscosity, yield point, and fluid loss control. Nanomaterials are thermally stable and can stabilize drilling fluid rheology at higher temperatures. Nanomaterials may increase WBMs HPHT performance.[42] Pressure and temperature can have complicated effects on the rheology of mud.[43] Mud system stability

was measured by the temperature at which a fluid may be exposed for 16 hours without losing more than half its viscosity.[44] Stable viscosity at high temperatures suggests that NPs may prevent viscosity from decreasing, exhibiting stable rheological behavior throughout a range of temperatures.[10] The desired rheological properties for the drilling fluid are a higher yield point and a lower plastic viscosity.[45]

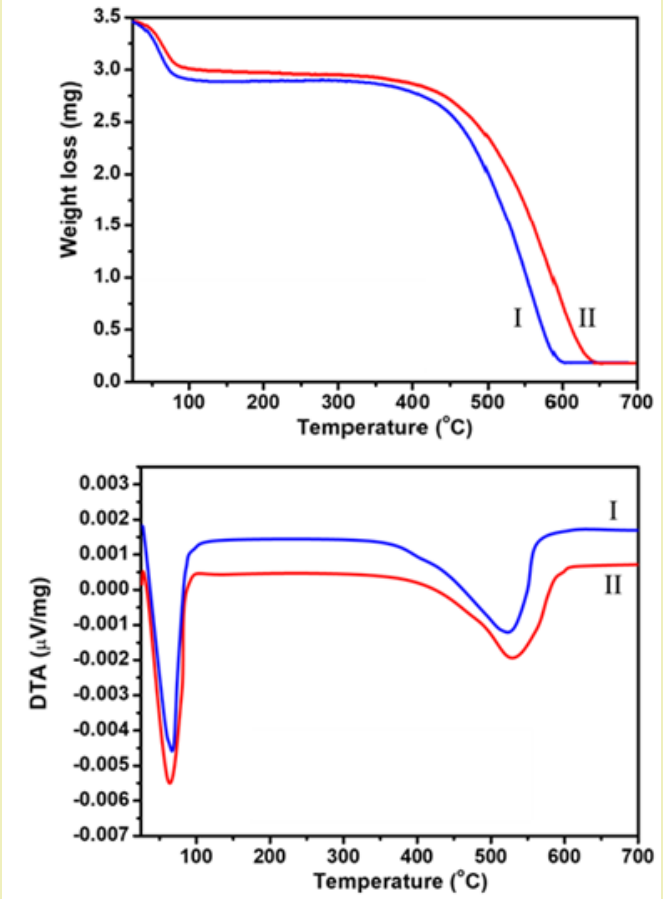

Figure 6: [Top] TGA and [Bottom] DTA thermograms for the prepared [I] Boron nitride nanoparticles modified graphene and [II] Boron nitride / titanium nitride modified graphene nanocomposites

Plastic viscosity (PV). Figure7A below illustrates how the HPHT conditions affect the PV of the mud fluids. Plastic viscosity is the total friction of the liquid and solid components in a drilling mud system and represents the overall resistance to fluid movement.[10] Increasing plastic viscosity reduces drilling penetration. High temperatures reduce the protective effect of mud fluid additives on bentonite clay. High plastic viscosity reduces drilling mud pumpability, increases pump pressure expenses, and could decrease efficiency.[45] As the temperature increases, plastic viscosity decreases. In contrast, the value of plastic viscosity increases as pressure increases.[46] The samples were showed a decrease in PV values due to high temperature effect.[47] This results from the attractive forces between the mud particles being thermally degraded.[48] However, nano-enhanced samples showed less reduction compared to blank one. This is caused by the rGB nanocomposite's increased surface area to volume ratio when compared to the clay particle ones, which increases internal contact and friction and raises the viscosity of the samples when compared to blank ones.[46] However, the amount of decrease for each nanocomposites ratio were found to be different.

Yield point (YP). YP is defined as the stress required to move a fluid or the fluid's resistance to flow. This indication shows how effectively the mud system can transport drilling cuttings from the borehole to the surface.[19] In order for the original fluid to flow, the shear stress must be greater than a critical value.[49] The YP is produced by the electrochemical attractive forces between the colloidal solid in the drilling fluid.[42,47] The yield point for blank mud, S1,S2 and S3 Samples decreased with increasing temperatures and pressures as shown in Figure 7B, reaching a minimum value at (200° C, 14000 psi). After which, there was a slight rise in the yield point at a pressure value of 170000 psi and temperature of 230 °C. also muds with nano composites revealed less reduction in YP compared to nano free sample. This suggests that because of the high thermal conductivity of NPs, which promotes heat dissipation by the drilling fluid and reduces the impacts of thermal degradation, enhanced muds containing nanocomposites are more resistant to temperature and pressure increases than base muds. Therefore, particularly at higher temperatures, strong thermal stability of NPs may aid in promoting YP of drilling muds.[47] The results showed that, in comparison to other samples and the blank sample at all pressures and temperatures, the S3 nanocomposite is a superior choice for maintaining the YP of mud.

Gel Strength (10-sec, 10 min). The measurement of electrochemical forces in the drilling fluid under static conditions is known as GS. It shows how effectively drilling cuttings and particles may be suspended in mud during times of no circulation.[42,48,50] In comparison to a blank sample, Figure 7C,D illustrates how changing temperature and pressure affect the suggested mud samples' 10-sec and 10-min gel strengths. It is evident from this chart that gel strength decreased as pressure and temperature increased. High GS is the result of increasing pressures.[51] However, a high temperature will increase intermolecular distances, which will reduce the fluid's flow resistance and, as a result, reduce the gel strength of the fluid.[43] The results confirms that the temperatures effects are more apparent than pressures.

Flow behavior. Drilling fluid flow behavior is best described by the relationship between shear stress and shear rate. Since the shear stress specifies the pumping properties of the drilling fluid, it is examined at different shear rates and high-temperature, high-pressure circumstances. When the particles are linked together at low shear rates, the flow resistance increases; when the connecting bonds are broken at high shear rates, the fluid behaves more like water.[45] The rheological models for different mud designs under HPHT conditions are compared in Figure 8. (A to D). Flow curve analysis was used to examine the developed drilling fluid system's flow behavior. For the purpose of examining the created drilling fluid

system's flow properties at high pressures and temperatures, flow models were fitted to experimental data from the viscometer. The experimental data obtained on the flow curve are fitted Herschel-Bulkley flow models at (80 C, 2000 psi). As the temperatures and pressures starts to increase altogether, the flow curve line starts to behave power low model and to some extend newtonian fluids curve for the rest of the proposed HPHT condition applied. The created drilling fluid formulation's viscosity vs. shear rate graph Figure 8 (A to D) shows a decrease in viscosity at higher shear rates, further validating the greater shear thinning behavior. The existence of flexible biopolymer segments in the nanocomposite polymer matrix might be the cause of this behavior.[52]

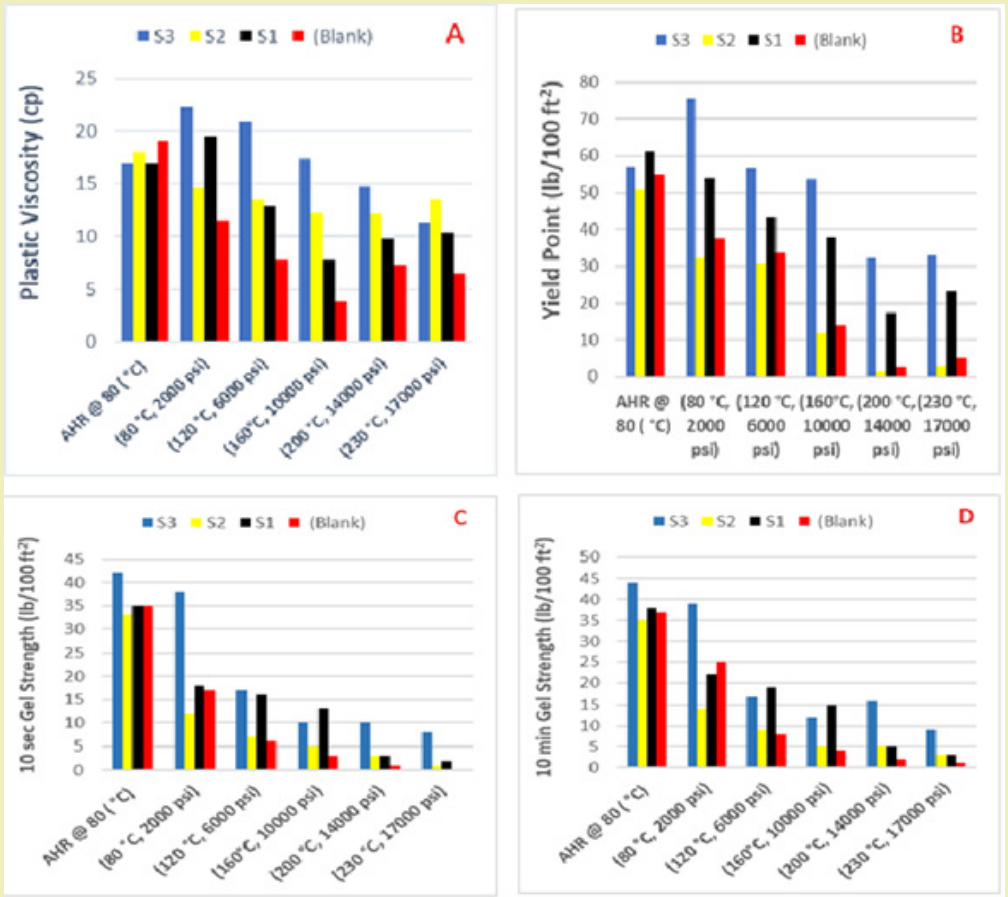

Figure 7: Drilling fluid rheology (with and without rGB nanocomposites) at HPHT conditions

- *Effect of rGBT nanocomposite components ratios on the rheological properties of WBM*

When compared to the reference mud at a 0.2% concentration, the newly formed nanocomposite had no effect on MW. This is due to fact that the additives are light in weight, and have a low specific gravity. The effects of rGBT nanocomposite components ratios Table 1 with a concentration of 0.2 wt.% on PV, YP, and 10 sec–10 min gel strength at HPHT conditions are shown clearly in Following figures.

Plastic Viscosity (PV). Reduction trend was observed with the elevation of temperature and pressure for all samples enhanced with the proposed nanocomposite Figure 9. The increased kinetic or thermal energy causes the liquid mobility to increase when the temperature increases to a particular degree. On the other hand, less binding force will result in a lower viscosity.[42] Blank and R3, R4, R6 samples showed slight reduction and degraded at 120 C, 6000 psi with 60%, 56%, 66 % and 55 % reduction respectively . While R1 and R2 samples degraded at 80C, 2000 psi and showed 65% and 53% reduction in PV relative to blank sample respectively. PV of sample S5 reduced only by 36 %. After which, all the above mentioned samples were almost continued to decrease with the elevated temperatures and pressures up to 160 C, 10000 psi followed by a slight increase due to high pressure effect toward the final applied HPHTs. This demonstrates the exceptional abilities of (R5) rGBT nanocomposite, which contains 60% r FLGO, 20% BN, and TiN nanoparticles to provide stable colloidal mechanisms to clays when mixed. This effectively prevents clays from flocculating in water, providing a significant amount of stability to the drilling fluids under HPHT conditions.

Yield point (YP). Figure 10. illustrates that the yield point for the rGBT nanocomposite muds were generally decreasing with increasing temperature and pressure until a temperature 200^{0}C, 14000 psi at which the YP declined suddenly to minimum values for the rest of the applied pressures and temperatures. Blank sample was generally decreased and degraded by 75 % with temperatures and pressures at 160 C, 10000 psi at which the YP dropped to a

minimal value at 200 C, 14000 psi. Whereas, R1 and R5 showed a slight increase in YP at 80 C, 2000 psi due to high pressure effect at low temperatures.[46] After which R1, R2,R3 and R4 were degraded at 200 C, 14000 psi by 73 %, 60 %, 68 % and 64 % reduction respectively compared the blank one. R5 and R6 were the only thermally stable samples as they recorded only 31% and 44 % reduction in PV respectively as they consider more than half of their original value.

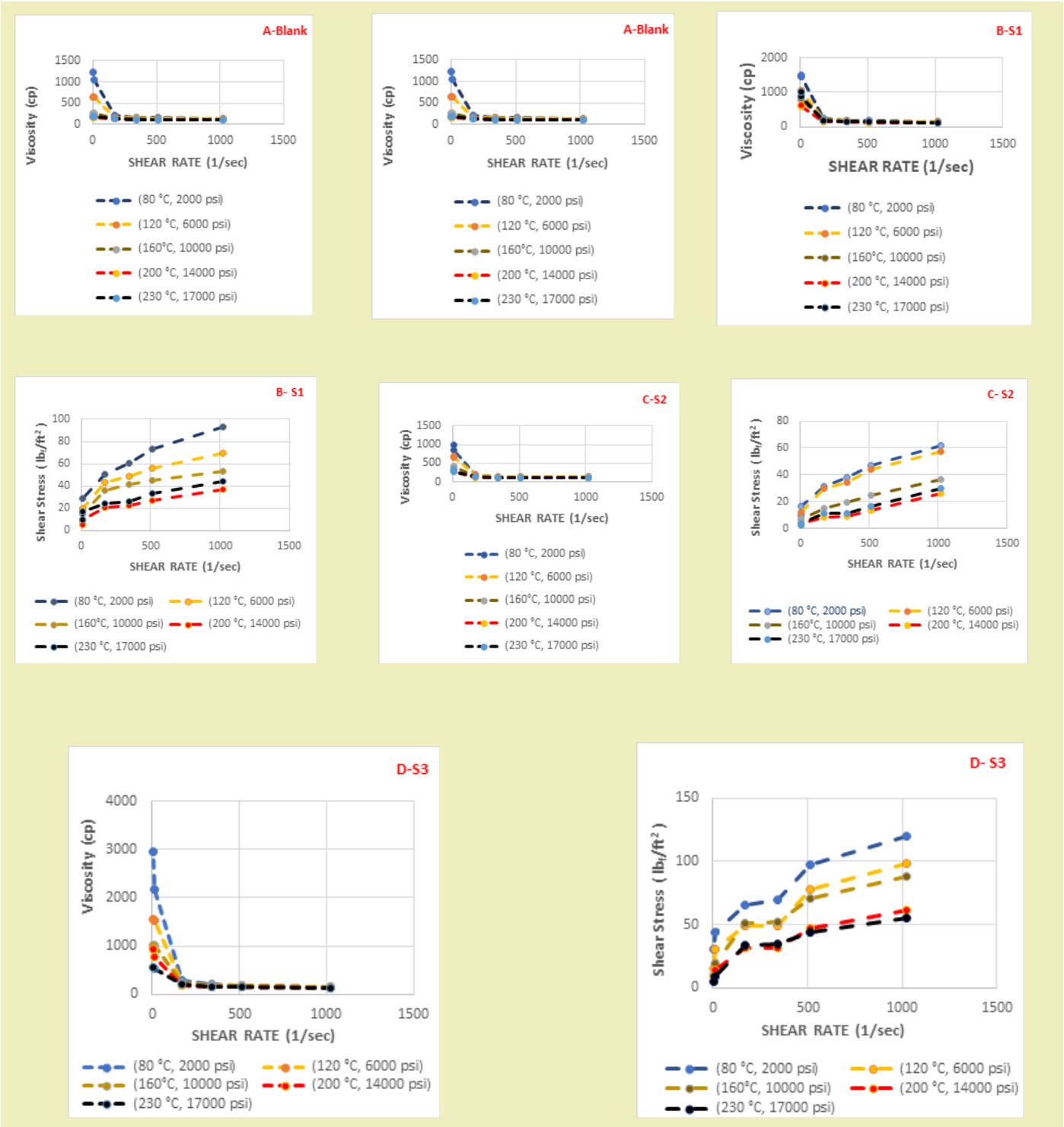

Figure 8: Effect of HPHT on the flow behavior of the developed drilling fluid formulation with rGB nanocomposites

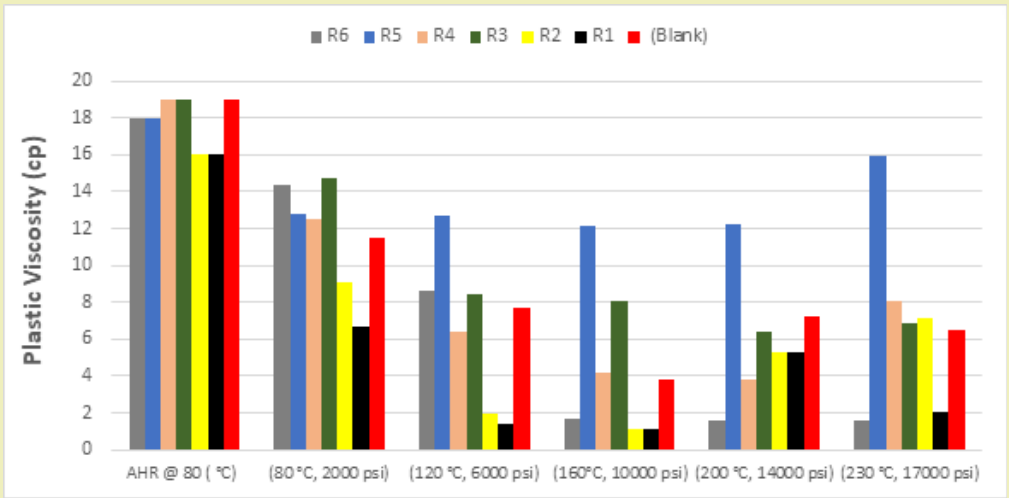

Figure 9: Comparative analysis of plastic viscosity at different aging temperatures at different pressures and temperatures

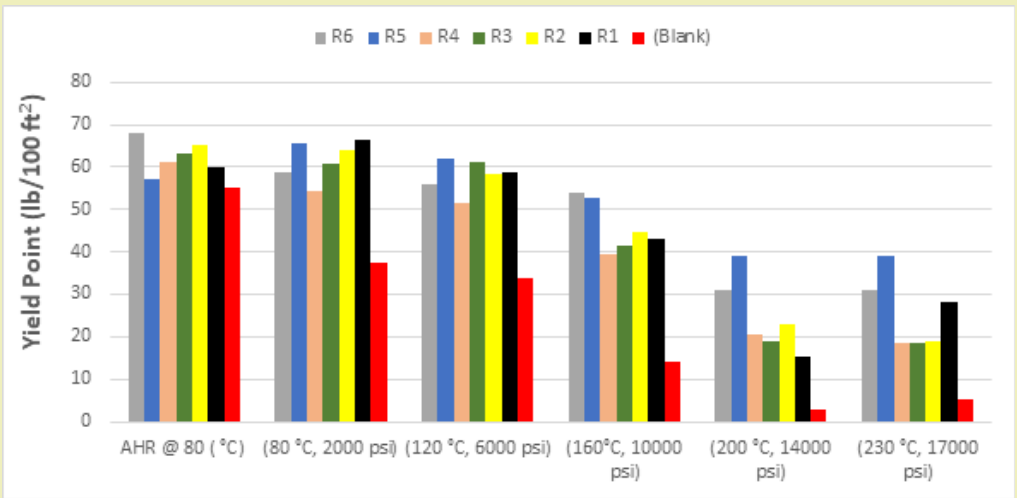

Figure 10: Comparative analysis of yield point at different aging temperatures at different pressures and temperatures

10 sec, 10 min gel strength (GS). Figure 11 and 12 shows the effect of varying temperature and pressure on 10-sec gel strengths of blank and six rGBT nanocomposite samples. Any additives that yield the low and flat gel strength with time were the optimal because they indicate that the gel strength value will not grow further over time and that it is sufficient to maintain the cutting in suspension under static conditions.[53] For the best drilling operation, the 10 sec and 10 min gel values must demonstrate fragile gelation. This is because this gelation ensures that no excessive shear force will be needed to break the gel again into the fluid when drilling operations restart.[48] The material gel strength increased with the pressure.[51] Obviously, reference sample gel strength increased when the prepared nanocomposites were added after hot roll aging AHR @ 80°C. After which, the gel strength was decreased sharply with increasing temperature and pressure for the reference mud until it reaches close to zero value at (200°C, 14000 psi). Additionally, It was also observed that the 10 sec, 10 min GS of all the mud samples enhanced with rGBT nanocomposites is higher than that of the reference set. Additionally, gel strength decreased with increasing mud temperature and pressure from 80°C, 2000 psi to 230°C, 17000 psi. The data also imply that this nanocomposite stabilizes gel strength better at increased temperatures and pressures, as demonstrated in all samples improved with it. Thus, rGBT preserves gel strength better in drilling fluids with harsh HPHT conditions.

Flow behavior. The observed shear stress of rGBT nanocomposites as a function of shear rate, temperature, and pressure is shown in Figure 13. (R1 to R6). It is clear that the experimental results, particularly at (80°C, 2000 pressure), closely match the Herschel-Bulkley fit. Shear stress decreases and flow curves follow power low model and, to some extent, Newtonian fluid curves when temperatures and pressures start to rise altogether. This is a sign that the mud is degrading. At low shear rates, the mud sample exhibits shear thinning behavior; at high shear rates, it grows more linearly.

Comparing the rheology of the nanocomposites

The rheological characteristics of the mud samples respond differently at high temperatures due to the expansion of the

molecules and the thermal degradation of the solid, polymers, and other components. As a result, the fluid's viscosity, yield point, and gel strength decrease along with its resistance to flow. Conversely, the molecules in the mud are compressed by high pressure. This explains why at higher pressure levels there is an increase in viscosity, yield point, and gel strength. Technically, it seems that the reference sample were degraded at 120°C, 6000 psi in terms of PV and GS as all the curves of PV and GS have undergone abrupt changes in behavior at this point. Whereas, at 160 °C, 10000 psi for its YP values. S1 Sample enhanced with rGB nanocomposite was failed at 160°C, 10000 psi. However, S2 and S3 were the thermally stable since they obtained more than half of their original set until the elevated applied HPHT conditions at 230°C, 17000 psi considering S3 was the highest, which was, contain 80% FLRGO and 20% BN.

Second samples were enhanced with rGBT nanocomposites, R3,R4 and R6 all were degraded for their PV at 160°C, 10000 psi . Abrupt changes in behavior were seen in R1 and R2 at 120°C, 6000 psi. Regarding YP, samples R1,R2, R3 and R4 all were failed at 200 C, 14000 psi. 10 sec, 10 min gel showed a continuous reduction trend along the elevated temperatures and pressures. R5 and R6 revealed their thermal stability in terms of rheological properties with the preference of R5. R5 with 60% FLRGO, 20% BN and 20% TiN would be the optimum option for the rest part of the study.

By extrapolating and comparing the rheological results obtained from the two nanocomposites relative to the reference mud. S3 would be the best option for rGB nanocomposite and R5 for rGBT nanocomposite. Therefore, R5 was the best. The rest of this work is investigating R5 at 0.6 wt% and 1 wt. % concerning rheological and filtration properties since all the a above mentioned works were done at 0.2 wt.% concentration.

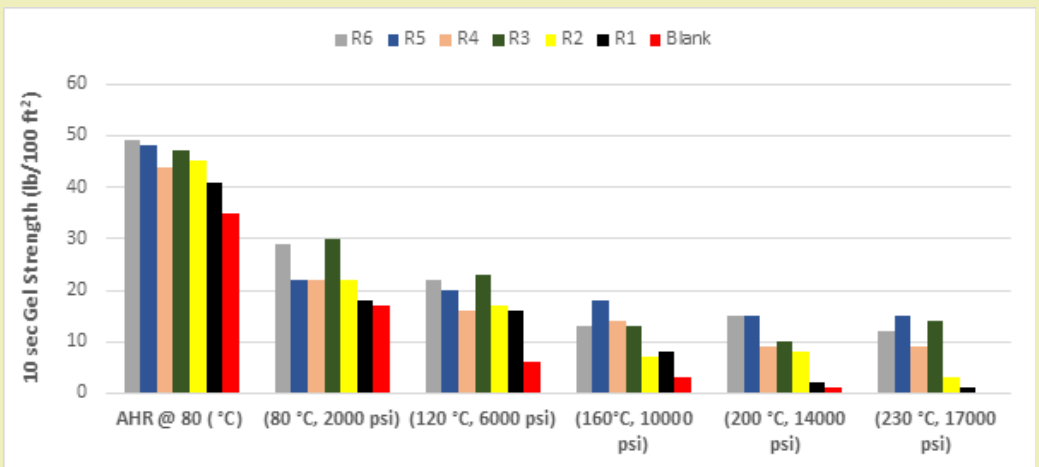

Figure 11: Comparative analysis of 10 sec gel strength at different pressures and temperatures

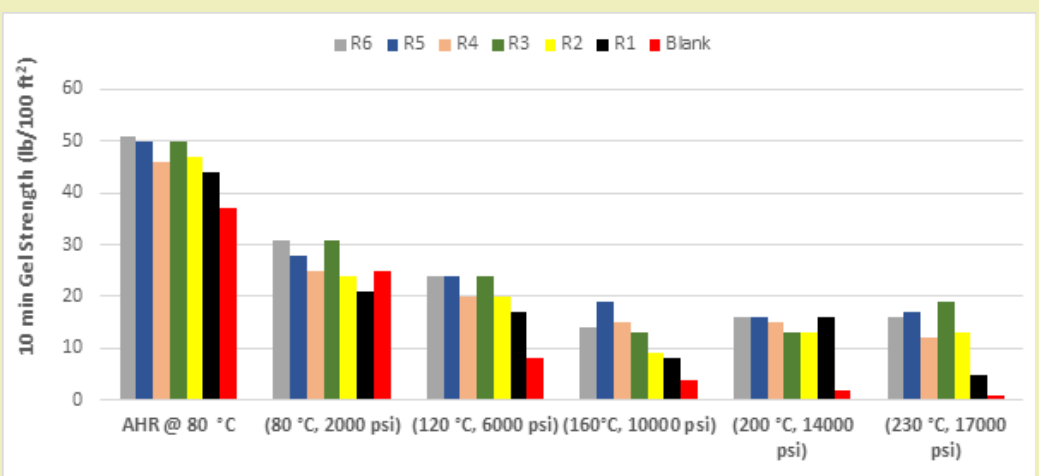

Figure 12: Comparative analysis of 10 min gel strength at different pressures and temperatures

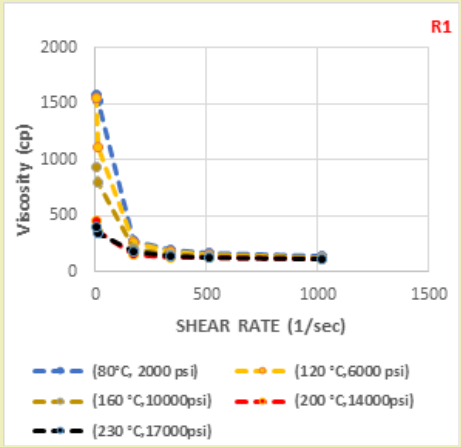
R1
Viscosity (cp)
SHEAR RATE (1/sec)
(80°C, 2000 psi)
(120 °C,6000 psi)
(160 °C,10000psi)
(200 °C,14000psi)
(230 °C,17000psi)

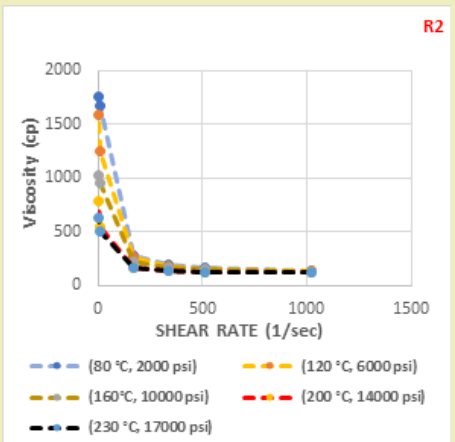
R2
Viscosity (cp)
SHEAR RATE (1/sec)
(80 °C, 2000 psi)
(120 °C, 6000 psi)
(160°C, 10000 psi)
(200 °C, 14000 psi)
(230 °C, 17000 psi)

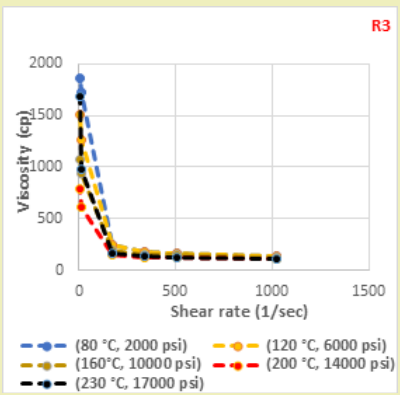
R3
Viscosity (cp)
Shear rate (1/sec)
(80 °C, 2000 psi)
(120 °C, 6000 psi)
(160°C, 10000 psi)
(200 °C, 14000 psi)
(230 °C, 17000 psi)

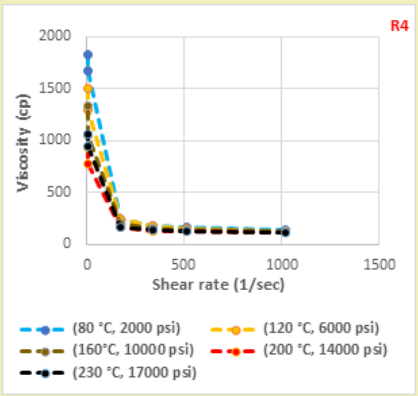
R4
Viscosity (cp)
Shear rate (1/sec)
(80 °C, 2000 psi)
(120 °C, 6000 psi)
(160°C, 10000 psi)
(200 °C, 14000 psi)
(230 °C, 17000 psi)

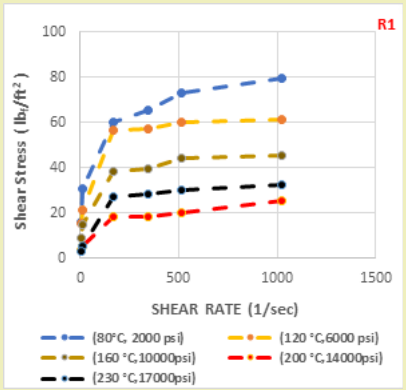
R1
Shear Stress (lb$_f$/ft^2)
SHEAR RATE (1/sec)
(80°C, 2000 psi)
(120 °C,6000 psi)
(160 °C,10000psi)
(200 °C,14000psi)
(230 °C,17000psi)

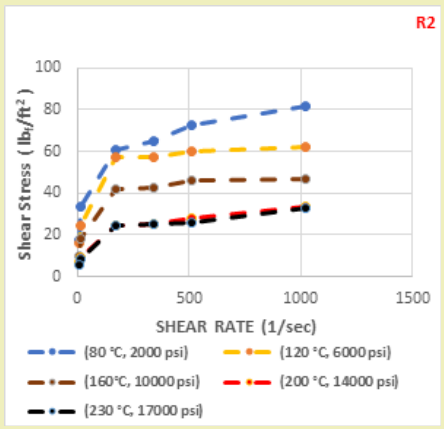
R2
Shear Stress (lb$_f$/ft^2)
SHEAR RATE (1/sec)
(80 °C, 2000 psi)
(120 °C, 6000 psi)
(160°C, 10000 psi)
(200 °C, 14000 psi)
(230 °C, 17000 psi)

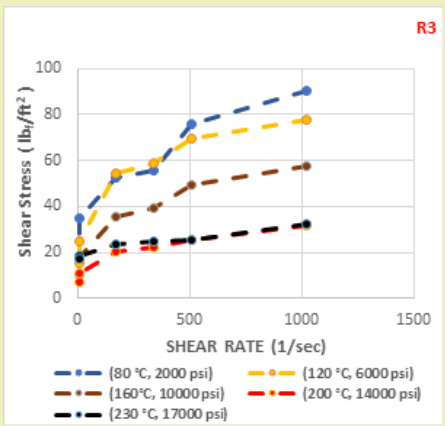
R3
Shear Stress (lb$_f$/ft^2)
SHEAR RATE (1/sec)
(80 °C, 2000 psi)
(120 °C, 6000 psi)
(160°C, 10000 psi)
(200 °C, 14000 psi)
(230 °C, 17000 psi)

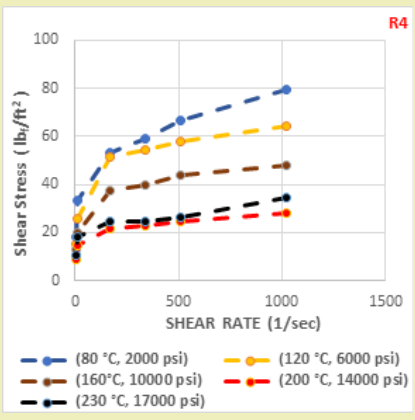
R4
Shear Stress (lb$_f$/ft^2)
SHEAR RATE (1/sec)
(80 °C, 2000 psi)
(120 °C, 6000 psi)
(160°C, 10000 psi)
(200 °C, 14000 psi)
(230 °C, 17000 psi)

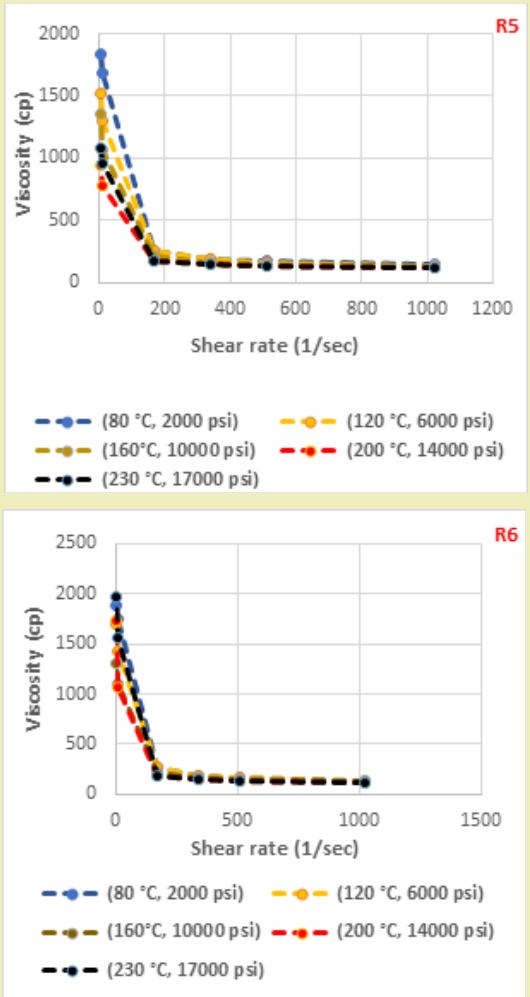

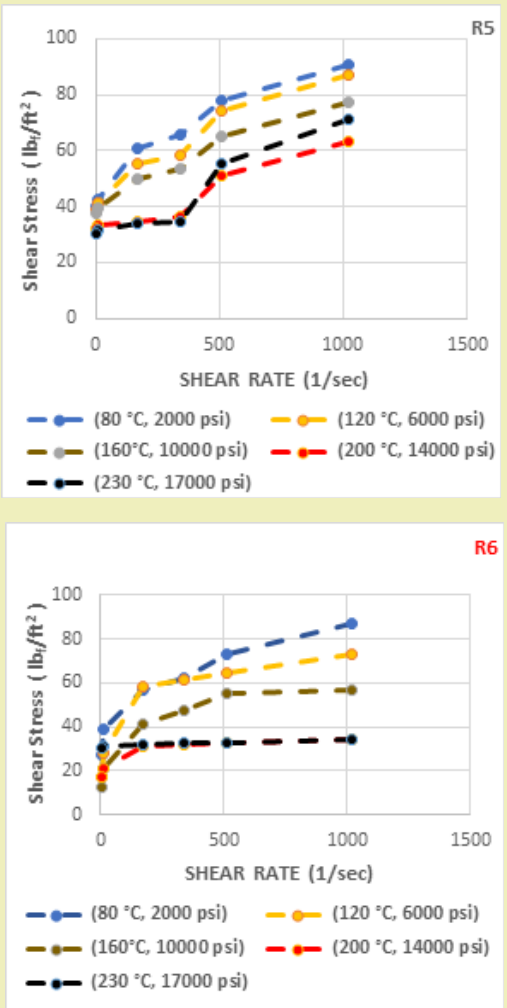

Figure 13: Effect of HPHT on the flow behavior of the developed drilling fluid formulation with rGBT nanocomposites

Effect of rGBT (R5) nanocomposite on the rheological and filtration properties of WBM at 0.6 and 1 wt.%

Rheological properties

Data represented in Figure 14A. shows that after different pressures and temperatures of various drilling fluid systems, the PV of all drilling fluids were decrease for proposed pressures and temperatures until (160°C,10000 psi), this is due to the thermal degradation of attractive forces among the mud particles. The PV of base mud was close to 8 cP, while after the addition of 0.2,0.6 and 1 % of rGBT(R5) additive in base mud, the PV of resulting drilling fluid was increased to 12,14,16 cP respectively at (200°C,14000 psi) and 15,16,19 cp at (230°C,17000 psi). Meaning that, as the concentration increase, PV would increase accordingly.

Figure 14B shows that the YP of drilling mud almost increased after the addition of 0.2, 0.6 and 1 % r GBT respectively in based mud as the pressures and temperatures increased to (160°C, 10000 psi) compared to blank sample. This is due to larger surface area and smaller size of rGBT, the electrostatic force of attraction among the mud particles is also increased. While after that, YP decreased slightly due to temperature effect but still higher than blank sample. The three concentration showed a reasonable thermal stability for (230°C, 17000 psi). The YP of base mud was 3 lb/100 ft² at (200°C, 14000 psi). While, after the addition of r GBT nanocomposite at 0.2, 0.6, 1 wt.%, the YP values were 39, 41 and 41 lb/100 ft² at (200°C, 14000 psi) and (230°C, 17000 psi) respectively. This modified viscosity of drilling mud obtained after the use of 0.2, 0.6, 1 % r GBT in the base mud would be supported in the lifting of drilling cutting from the bottom hole to the surface during the drilling operations.

The GS acquired at various temperatures and pressures illustrates in Figure 14C,D The result demonstrates that the addition of 0.2, 0.6 and 1 wt.% nanomaterials reduced the 10sec and 10 min GS at HPHT condition. According to the result, at (80°C, 2000 psi), (120°C, 6000 psi), (160°C, 10000 psi), (200°C, 14000 psi) and (230°C, 17000 psi), the GS of mud sample with 0.2 wt.% nanomaterials reduced from 22 lb/100ft² , 20 lb/100ft2, 18 lb/100ft², 15 lb/100ft² and 15 lb/100ft². Resulting in a reduction of 55%, 59 %, 63 %, 69 % and 69 % for 10sec GS, respectively. As

for 10 min GS, a reduction of 44 %, 52 %, 62 %, 68 % and 66 % were observed. A similar decrease of 40%, 47%, 47%, 49%, and 44% for 10 seconds GS and 39%, 49%, 47%, 49%, and 45% for 10 minutes GS was seen in the mud sample containing 0.6 weight percent nanomaterials. The proper dispersion of nanomaterials in mud samples as temperatures increase leads to a drop in attractive forces and an increase in repulsive forces between the solid particles, resulting in the production of a very fragile gel. This decrease in GS is the outcome. Because the drill string's first rotation causes the drilling fluid to circulate slowly, the brittle GS is desirable because it is prone to breaking. On the other hand, a high GS might need a greater pump rate to get the mud circulated again, which could cause formation fracture.[54] However, the addition of 1 wt. % nanomaterial results in progressive gel formation by increase GS compared to reference mud by about 63%, 87 %, 93 %, 97 and 99 % respectively at elevated temperatures and pressures. Finally, an increase also obtained by 50 %, 83 %, 90 %, 95 % and 97 % for 10 min GS respectively. Compared to the blank sample, an enhancement in GS where witnessed.

Since the shear stress specifies the pumping properties of the drilling fluid, it is examined at different shear rates and high-temperature, high-pressure circumstances. As a function of shear rate HPHT environments, the observed shear stress of WBM enhanced with rGBT(R5) nanocomposite at concentrations of 0.6 and 1% is shown in Figure 10. The inclusion of nanomaterial significantly lowers the shear stress of WBM at all pressures and temperatures, according to the results. The mud sample exhibits shear thinning behavior at low shear rates, while in the high shear rate range, it expands more linearly. In addition, the base mud sample shows lower yield stress than the nanofluids at both high and low temperature and pressure conditions. In contrast to the blank sample, which displays Newtonian flow behavior at high temperatures and pressures, the concentration-dependent flow behavior curves continue to follow the Herschel-Bulkley model. Additionally, the data demonstrate that viscosity dramatically reduces at low shear rates when pressure and temperature rise from 80°C and 2000 psi to 230°C and 17000 psi. Liquid mobility increases as a result of increased kinetic or thermal energy when temperature reaches a specific value. Nonetheless, the viscosity will decrease with a lower binding force.[55] All of the mud samples exhibit the pseudoplastic shear-thinning behavior, as shown by the data displayed in Figure 15. As the temperature, pressure, and shear rate increase, the mud sample's viscosity decreases. At lower shear rates, this phenomena was more pronounced. A high shear rate may result in the shear-thinning effect due to drilling fluid component degradation..[56] This behavior of drilling fluid at a high shear rate is essential for proper pumping operation and better hole cleaning.[57]

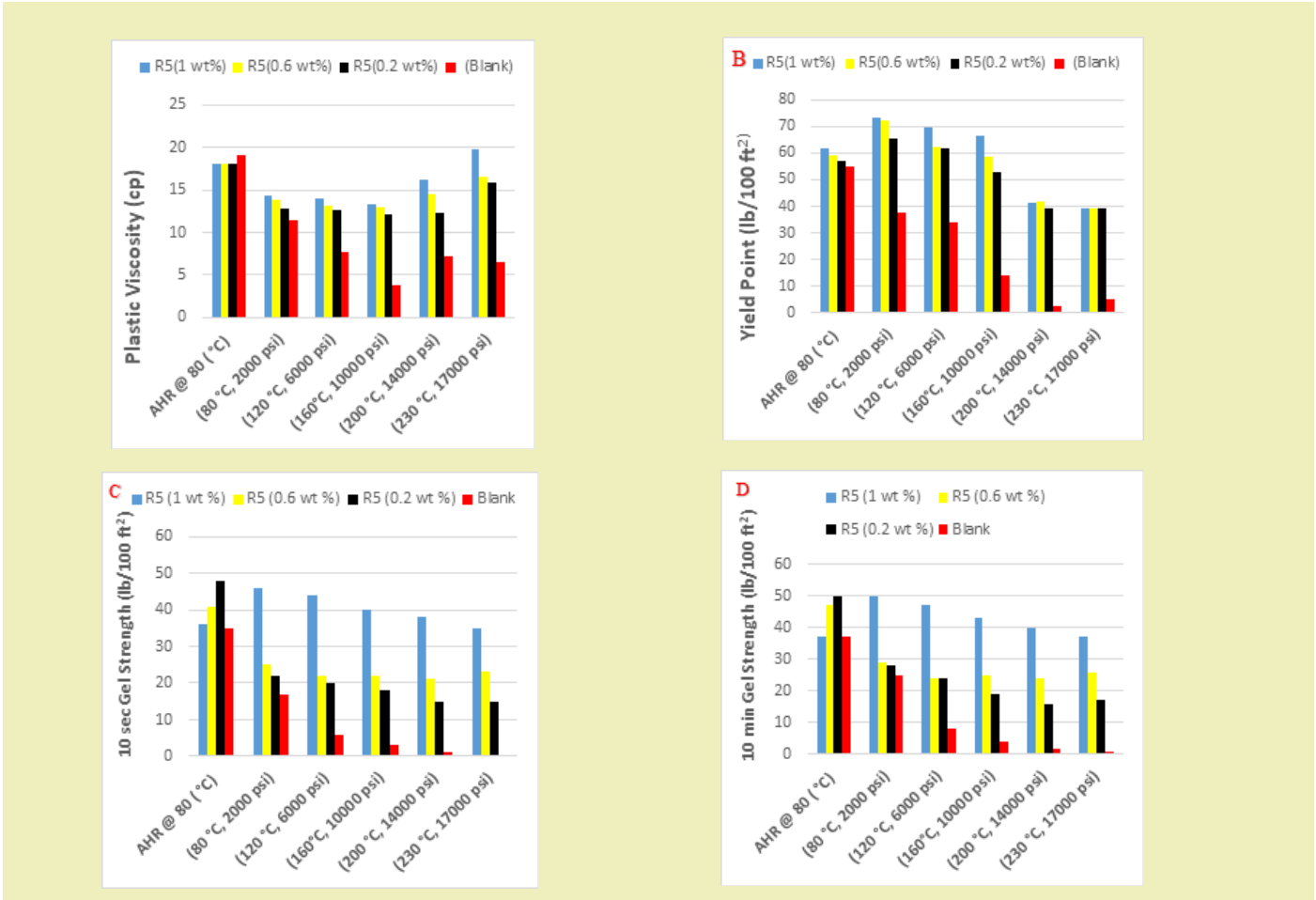

Figure 14: Rheological properties for blank and R5 sample with 0.2, 0.6 and 1 wt % at HPHT conditions

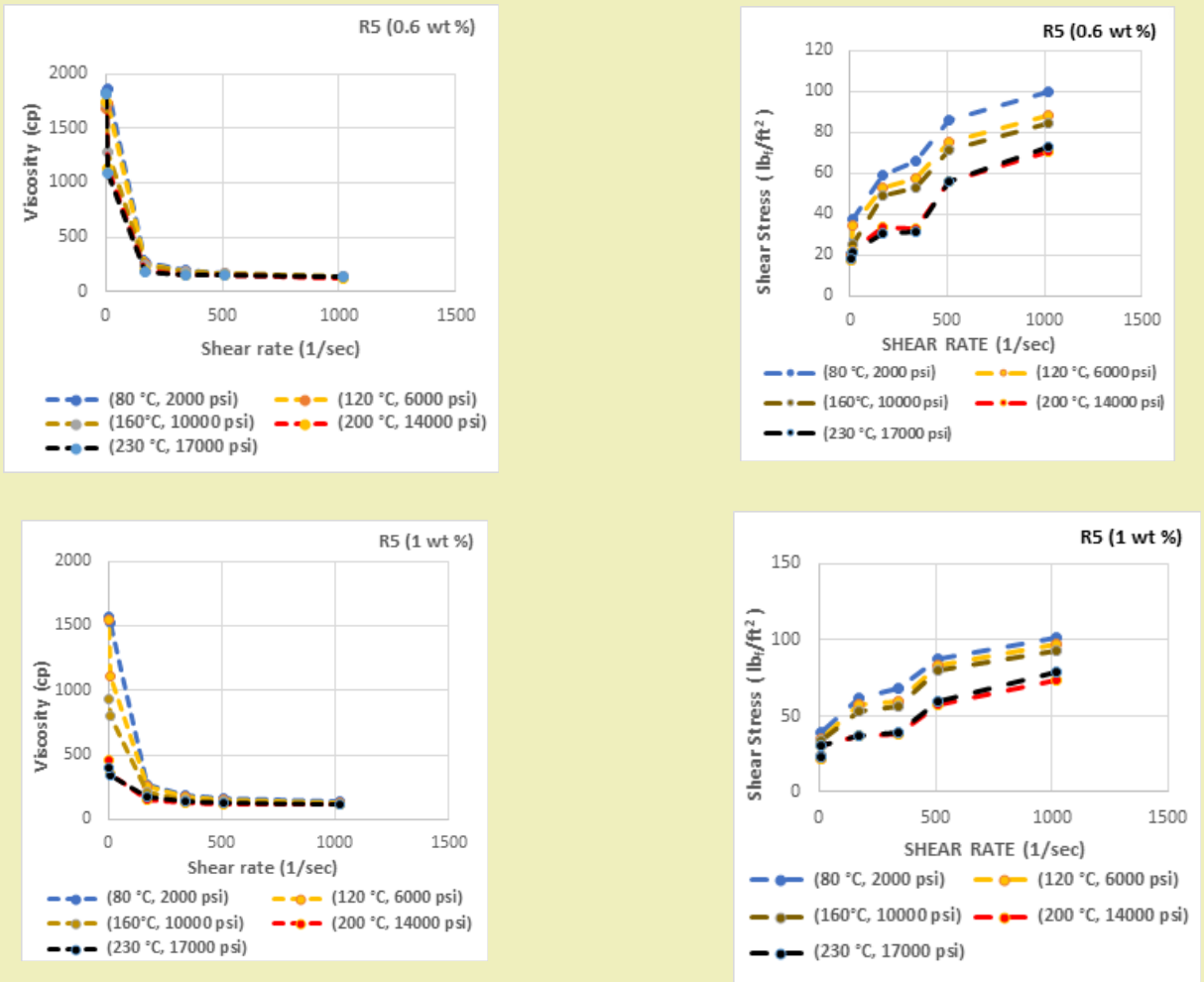

Figure 15: Flow behaviour of R5 sample at 0.6 and 1 wt % at HPHT conditions

Filtration and filter cake thickness of WBM at HPHT condition

The filtration properties were assessed by experimental testing conducted under various pressure and temperature conditions. The investigation focused on the filtration properties, which were assessed by measuring factors such as the amount of filtration loss and the thickness of the mud cake after a particular time period. The HPHT property for the reference sample was measured to be 44 mL after 30 minutes. The experimental findings obtained under high pressure, high temperature (HPHT) conditions for all the samples proposed in this study are depicted in Figure 16. Using rGB and rGBT nanocomposites at different concentrations is observed to gradually reduce the filtration loss volume up to 32 mL at 0.2 and 0.6 wt% concentration for R5 sample. Additionally, by including 1% of the GBT nanocomposite with sample R5, the filtering loss volume significantly decreased to 30 mL. The use of rGB and rGBT nanocomposites reduces filtering loss volume because they improve the electrostatic interactions between their negative ions and other particles, creating an appropriate suspended system that prevents particle flocculation. A thin layer of low-permeable mud cake might develop on the surface of the lost zone if well-suspended and deflocculated particles are mixed with drilling fluid.[58] The electrostatic attractive force between rGBT and other solid particles, such positive edge bentonite with negative face or edge rGBT, is the reason for such reduction in filtration. The rGBT and other particles that may form a gelling structure, which increases mud consistency and lowers mud filtration volume, were attracted to one other.[59] One important finding of utilizing rGBT nanocomposite in WBDF is that it lessens the likelihood of the drill string sticking during the drilling process when the thickness of the mud cake is reduced (mm). As shown in Figure 17, the majority of the 45% reduction in mud cake thickness was achieved by adding 1 wt.% of rGBT(R5) compared to the basic sample that did not include any nanomaterials. Whereas adding 0.2 and 0.6 wt.% decreased the cake thickness by 38 % and 40% respectively. Meaning that, as the concentration increase the filter volume and filter cake thickness decrease. Figurex. reveals the different filter cake for all the samples addressed in this study.

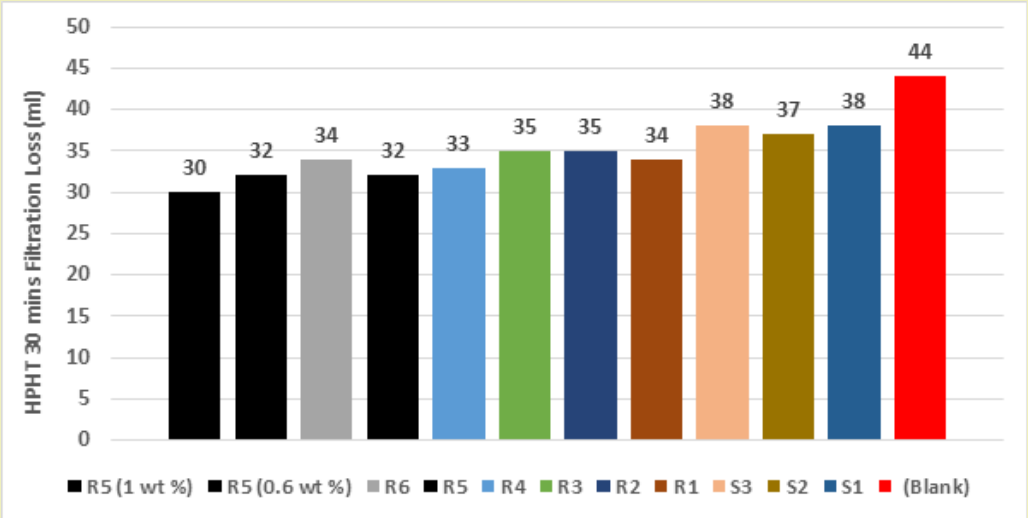

Figure 16: Filtrate volume for different mud samples at HPHT conditions

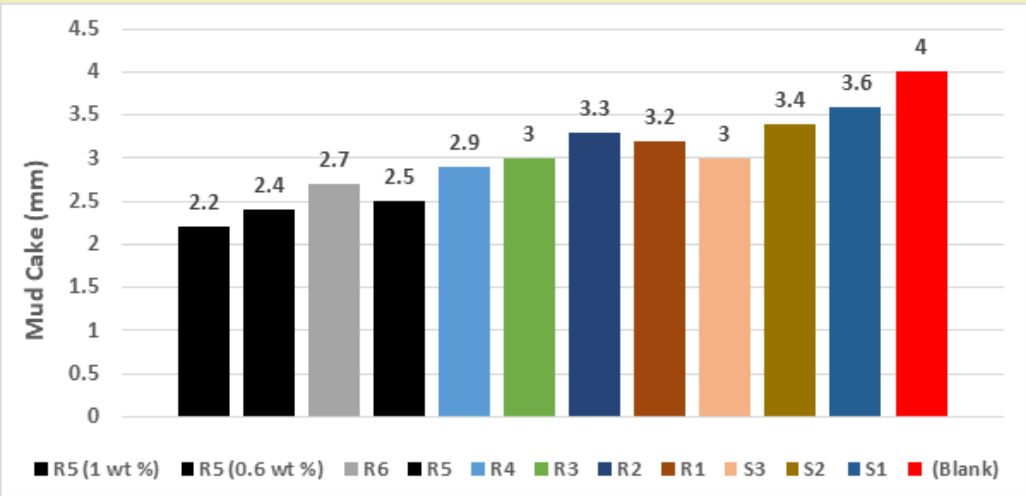

Figure 17: Filter cake thickness for different mud samples

Conclusion

This work successfully developed multifunctional drilling fluids by combining WBM with decorated FLRGO that contained BN / TiN nanoparticles. Three sets of FLRGO functionalized with BN and six sets of the same nanocomposite decorated with TiN nanoparticles but different in nano ratios were successfully prepared and characterized. SEM showed the successful exfoliation of compact graphene oxide layers and homogenous nanoparticles distribution as a result of efficient surface decoration of rGO with BN and TiN. Also, the cake micrographs exhibit fusion of the nanolayers with the mud composition. EDX displayed the presence of nanoparticles on the graphene surface and also in the mud sample. XRD exhibited slight shift in the main peaks of nanoparticles confirming the strong physical interaction between graphene surface and the guest nanoparticles. FTIR indicated the strong interaction within the nanocomposite matrix in terms of hydrogen bonding. TGA/DTA demonstrated the superior thermal properties of the graphene nanocomposite containing both nitrides nanoparticles. The chosen sample from r GB and r GBT nanocomposites was then examined in its 0.6 wt. and 1 wt. % concentration. The accompanied rheological and filtration properties were evaluated under the conditions of LPLT and HPHT conditions. Furthermore, the conditions under which water based mud of certain composition fails were determined. Based on the results of the tests performed, the following conclusions were made:

The rheological properties for both nanocomposites concerning PV, YP and GS were all improved and in HPHT conditions compared to blank sample. An increase in temperature and pressures altogether significantly reduces the PV, YP and GS of the mud samples. Changes in pressure have a less noticeable impact than changes in temperature.

S3 with 80 % FLRGO and 20 % BN and R5 with 60 % FLRGO, 20 % BN and 20 % TiN nanocomposites at 0.2 wt.% concentration were found to be the least affected nanocomposites at elevated HPHT conditions in terms of rheological properties, therefore they can be considered to have a high thermal stability. However, the sample R5 showed the lowest effect relative to reference sample. More rheological improvement were observed as the concentration of r GBT nanocomposite (R5) increased to 0.6 wt.% and 1 wt. %. Meaning that, as the concentration increases, the thermal stability would increase as well. As HPHT increased from 80 ◦C, 2000 psi to 230 ◦C, 17000 psi, PV with R5 was enhanced by 10 % to 59 % at (0.2 wt%), 17 % to 61 % at (0.6 wt.%) and 20 % to 67 % at (1 wt.%) respectively relative to reference mud. Similarly, yield point was enhanced by 44% to 88% at (0.2 wt%), 49 % to 88 % at (0.6 wt.%) and 50 % to 89 % at (1 wt.%) respectively relative to reference mud. The most improvement in gel strength property was observed with (1 wt.%) concentration since it recorded almost the same value as the original nanofree sample after exposing to the proposed HPHTs.

Both nanocomposites significantly decreased the filtrate loss under HPHT conditions, which enhanced the filtering properties of the WBMs. At HPHT conditions, the greatest reduction in filtrate loss occurs when R5 nanocomposite concentration is raised from 0.2 to 1 wt %. The viscosity of water-based muds is well-represented mathematically by the Herschel-Bulkley model, particularly at temperatures below the mud's failure point. Overall, the evaluated nanoparticles improved the rheological and filtration properties, which suggest their applicability of being used as rheology and filtration loss modifiers.

It is essential to remember that these results apply to the particular mud samples that were utilized in the research since they were derived from the observations collected over the course of the investigation. Although muds with various weights and formulas may react to changes in temperature and pressure somewhat differently, overall mud behavior is expected to be quite similar.

Acknowledgements

The authors would like to express their gratitude to Egyptian Mud Engineering and Chemicals Company (EMEC) for their kind help. This means providing materials for the research and helping with necessary laboratory measurements. We would also want to express our appreciation to the National Research Centre in Dokki, Egypt, for providing the laboratory facilities required to complete most of the studies and prepare the materials. Also, financial aid from National Research Centre under the grant number 13010307 (PI: Dr. Ahmed Ghanem) is highly appreciated for supporting synthesis of few layer reduced graphene oxide nanosheets.

Funding

This Research Article received no external funding.

Declaration of Competing Interest

The authors declare that they have no known competing financial interests or personal relationships that could have appeared to influence the work reported in this paper.

References

1. Hanyi Zhong WH, Guan Y, Su J, et al. Hydrothermal synthesis of bentonite carbon composites for ultra-high temperature filtration control in water-based drilling fluid. *Appl Clay Sci*. 2022;230:106699.
2. Amani A, Al jubouri M, Shadravan A. Comparative Study of Using Oil-Based Mud Versus Water-Based Mud in HPHT Comparative Study of Using Oil-Based Mud Versus Water-Based Mud in HPHT. *Egyptian Journal of Petroleum*. 2016;25(4):459-464.
3. Beg M, Kumar P, Choudhary P, et al. Effect of high temperature ageing on TiO2 nanoparticles enhanced drilling fluids : A rheological and filtration study. *Upstream Oil Gas Technol*. 2020;5:100019.
4. Aftab A, Ismail AR, Ibupoto ZH, et al. Nanoparticles based drilling muds a solution to drill elevated temperature wells : A review. *Renew Sustain Energy Rev*. 2017;76:1301-1313.
5. Sudharsan J. Behaviour of Drilling Fluids on HPHT Well Conditions. *IJASRM*. 2018;3(7):2-4.
6. Sean R Smith, Rafati R, Shari A, et al. Application of Aluminium Oxide Nanoparticles to Enhance Rheological and Filtration Properties of Water Based Muds at HPHT Conditions. *Colloids Surfaces A Physicochem Eng Asp*. 2017;537:361-371.
7. Mao H, Yang Y, Zhang H, et al. Conceptual design and methodology for rheological control of water-based drilling fluids in ultra-high temperature and ultra-high pressure drilling applications. *J Pet Sci Eng*. 2020;188(1):106884.
8. Abduo MI, Dahab AS, Abuseda H, et al. Comparative study of using Water-Based mud containing Multiwall Carbon Nanotubes versus Oil-Based mud in HPHT fields. *Egypt J Pet*. 2015;25(4).
9. Amani M, Al jubouri M. The Effect of High Pressures and High Temperatures on the Properties of Water Based Drilling Fluids. *Energy Science and Technology*. 2012;4(1):27-33.
10. Martin C, Babaie M, Nourian A, et al. Designing Smart drilling fluids using modified nano silica to improve drilling operations in Geothermal wells. *Geothermics*. 2023;107:102600.
11. Talukdar P. Study on the rheological properties of a novel drilling fluid for the pay zones of high pressure high temperature oil-wells. *IJARET*. 2021;12(2):303-312.
12. Mohamadian N, Ghorbani H, Wood D, et al. Advances in Rheological and filtration characteristics of drilling fluids enhanced by nanoparticles with selected additives: an experimental study. *Advances in geo-energy research*. 2018;2(3):228-236.
13. Azwadi N, Sidik C, Adamu IM, et al. Preparation Methods and Thermal Performance of Hybrid Nanofluids. *Journal of Advanced Research in Materials Science.* 2019;56(1):1-10
14. Sajjadian M, Sajjadian VA, Rashidi A. Experimental evaluation of nanomaterials to improve drilling fluid properties of water-based muds HP/HT applications. *J Pet Sci Eng*. 2020;190:107006.
15. Jia X, Zhao X, Chen B, et al. Applied Surface Science Polyanionic cellulose / hydrophilic monomer copolymer grafted silica nanocomposites as HTHP drilling fluid-loss control agent for water-based drilling fluids. *Appl Surf Sci*. 2022;578:152089.
16. Mohammed Zayan J, Rasheed AK, John A, et al. Investigation on Rheological Properties of Water-Based Novel Ternary Hybrid Nanofluids Using Experimental and Taguchi Method. *Materials (Basel)*. 2021;15(1):28.

17. Geng Y, Zhang Z, Yan Z, et al. A novel graphene/triolein complex-based lubricant for improving high temperature water-based drilling fluid. *RSC Adv*. 2023;13:34772-34781.
18. Yahya MN, Norddin MNAM, Ismail I, et al. Modified locally derived graphene nanoplatelets for enhanced rheological, filtration and lubricity characteristics of water-based drilling fluids Rate of Penetration. *Arab J Chem*. 2023;16(12):105305.
19. Rong L, Santra A, Ross G, et al. Grafted graphene oxide nanoparticles as a yield point enhancer in water-based drilling fluids. *Mater Today Chem*. 2023;34(3):101820.
20. Zhong H, Guan Y, Qiu Z, et al. Application of carbon coated bentonite composite as an ultra-high temperature filtration reducer in water-based drilling fluid. *J Mol Liq*. 2023;375:121360.
21. Luo T, Li J, Xu J, et al. The Effects of Organically Modified Lithium Magnesium Silicate on the Rheological Properties of Water-Based Drilling Fluids. *Materials (Basel).* 2024;17(7):1564.
22. Ahmed A, Pervaiz E, Abdullah U, et al. Optimization of Water Based Drilling Fluid Properties with the SiO2/g-C3N4 Hybrid. *ACS Omega*. 2024;9(13):15052-15064.
23. Ghanem F, Yassin MA, Cosquer R, et al. Polycaprolactone composite films infused with hyperbranched polyester/reduced graphene oxide: influence on biodegradability, gas/water transport and antimicrobial properties for sustainable packaging. *RSC Adv*. 2024;14(9):5740-5753.
24. API. Recommended practice for laboratory testing of drilling fluids-13I. *Api Recomm Pract*. 2009;8:124.
25. Ghanem AF, Abdel Rehim MH. Assisted Tip Sonication Approach for Graphene Synthesis in Aqueous Dispersion. *Biomedicines.* 2018;6(2):63.
26. Türkez H, Arslan ME, Sönmez E, et al. Synthesis, characterization and cytotoxicity of boron nitride nanoparticles: emphasis on toxicogenomics. *Cytotechnology.* 2019;71(1):351-361.
27. Singh B, Kaur G, Singh P, et al. Nanostructured Boron Nitride With High Water Dispersibility For Boron Neutron Capture Therapy. *Sci Rep*. 2016;6:35535.
28. Locovei C, Chiriac AL, Miron A, et al. Synthesis of titanium nitride via hybrid nanocomposites based on mesoporous TiO2/acrylonitrile. *Sci Rep*. 2021;11(1):1-9.
29. Gray BM, Hector AL, Jura M, et al. Effect of oxidative surface treatments on charge storage at titanium nitride surfaces for supercapacitor applications. *J Mater Chem A*. 2017;4550-5:4559.
30. Mahdizadeh A, Farhadi S, Zabardasti A. Microwave-assisted rapid synthesis of graphene-analogue hexagonal boron nitride (h-BN) nanosheets and their application for the ultrafast and selective adsorption of cationic dyes from aqueous solutions. *RSC Adv*. 2017;7:53984-53995.
31. Tran DT, Nguyen VN. RGO/persulfate metal-free catalytic system for the degradation of tetracycline: Effect of reaction parameters. *Mater Res Express*. 2020;7(7):1-12.
32. Zalan Z, Lazar L, Fulop F. Chemistry of Hydrazinoalcohols and their Heterocyclic Derivatives. Part 1. Synthesis of Hydrazinoalcohols. *Curr Org Chem*. 2010;7(4):357-376.
33. Schniepp HC, Li JL, McAllister MJ, et al. Functionalized single graphene sheets derived from splitting graphite oxide. *J Phys Chem B.* 2006;110(17):8535-8539.
34. Mattevi C, Eda G, Agnoli S, et al. Evolution of electrical, chemical, and structural properties of transparent and conducting chemically derived graphene thin films. *Adv Funct Mater*. 2009;19(16):2577-2583.
35. Al Jabbari YS, Koutsoukis T, Al Hadlaq S, et al. Surface and cross-sectional characterization of titanium-nitride coated nickel-titanium endodontic files. *J Dent Sci.* 2016;11(1):48-53.
36. Ahmed F. Ghanem and Mohamed A, et al. Investigation of water sorption, gas barrier and antimicrobial properties of polycaprolactone films contain modified graphene. *J Mater Sci*. 2021;56(1):497-512.
37. Mustafa M Alezzi, Ahmed F Ghanem, Abdel Alim H El Sayed, et al. Fabrication of Graphene Oxide/ Boron Nitride / Titanium Nitride Nanocomposites for Improving Performance of Water Based Drilling Fluids in Low-Pressure Low-Temperature Wells. *Egyptian Journal of Chemistry.* 2024;67(13):2197-2205.
38. Bayon NN. Synthesis and characterization of titanium nitride nanoparticles. *Materials Express.* 2022;12(9):1211-1215.
39. Gebreegziabher GG, Asemahegne AS, Ayele DW, et al. One-step synthesis and characterization of reduced graphene oxide using chemical exfoliation method. *Mater Today Chem*. 2019;12:233-239.
40. Xu W, Li A, Liu Y, et al. CuMoO4@hexagonal boron nitride hybrid: an ecofriendly flame retardant for polyurethane elastomer. *J Mater Sci.* 2018;53:11265-11279.
41. Yoo JB, Yoo HJ, Jung HJ, et al. Titanium oxynitride microspheres with the rock-salt structure for use as visible-light photocatalysts. *J Mater Chem A.* 2016;4(3):869-876.
42. Arain H, Ridha S, Mohyaldinn ME, et al. Improving the performance of invert emulsion drilling fluid using boron nitride and graphene nanoplatelets for drilling of unconventional high-temperature shale formations. *J Mol Liq*. 2022:363:119806.
43. Amani M, Texas A, Al jubouri M, et al. SPE 157219 An Experimental Investigation of the Effects of Ultra-High Pressure and Temperature on the Rheological Properties of Water-Based Drilling Fluids. 2012.
44. Howard SK. Formate Brines for Drilling and Completion: State of the Art. 1995;pp.1-14.
45. Ajienka AJ, Okon AN, OSOKOGWU U. Evaluating the Effects of Additives on Drilling Fluid Characteristics. *IJESRT*. 2014;3(6).
46. Amani M, Al Jubouri M. The Effect of High Pressures and High Temperatures on the Properties of Water Based Drilling Fluids. *Energy Sci Technol*. 2012;4(1):27-33.
47. Esfandyari B, Harati S, Kolivandi H. Evaluation of rheological and filtration properties of a polymeric water-based drilling mud in presence of nano additives at various temperatures. *Colloids Surfaces A Physicochem Eng Asp*. 2021;627:127128.
48. Prakash V, Sharma N, Bhattacharya M. Effect of silica nano particles on the rheological and HTHP filtration properties of environment friendly additive in water based drilling fluid. *J Pet Explor Prod.* Technol. 2021;(12):4253-4267.
49. Rafati R, Smith SR, Shari A, et al. Effect of nanoparticles on the modi fi cations of drilling fl uids properties : A review of recent advances. *Journal of Petroleum Science and Engineering.* 2018;161:61-76.
50. Bayat E, Jalalat Moghanloo P, Piroozian A, et al. Experimental investigation of rheological and filtration properties of water-based drilling fluids in presence of various nanoparticles. *Colloids Surfaces A Physicochem Eng Asp.* 2018;555:256-263.
51. Andrade RV, Galdino JF, Franco AT, et al. Influence of pressure on the gel strength and on the solid-like behavior for an inverted emulsion drilling fluid. *Journal of Petroleum Science and Engineering.* 2022;219:111114.
52. Jain R, Mahto TK, Mahto V. Rheological investigations of water based drilling fluid system developed using synthesized nanocomposite. *Korea Aust Rheol J*. 2016;28(1):55-65.

53. Elkatatny S, Kamal MS, Alakbari F, et al. Optimizing the rheological properties of water-based drilling fluid using clays and nanoparticles for drilling horizontal and multi-lateral wells. *Appl Rheol.* 28(4):1-8.

54. Elochukwu G, Gholami R, Dol SS. An approach to improve the cuttings carrying capacity of nanosilica based muds. *J Pet Sci Eng.* 2017;152:309-316.

55. Sulaimon AA, Adeyemi BJ, Rahimi M. Performance enhancement of selected vegetable oil as base fluid for drilling HPHT formation. *J Pet Sci Eng.* 2017;152:49-59.

56. Hasan S, Aghaei H, Ghabdian M. On the attributes of invert-emulsion drilling fl uids modi fi ed with graphene oxide / inorganic complexes. *J Ind Eng Chem.* 2021;93:290-301.

57. Ihekoronye KK, Izuwa NC, Ekwueme ST, et al. Evaluating the rheological property of Irvingia gabonensis and Abelmoschus esculentus as a substitute to conventional Pac R on cutting carrying capacity and hole cleaning. *J Pet Explor Prod Technol*. 2020;10(3):1069-1079.

58. Barry MM, Jung Y, Lee J, et al. Fluid filtration and rheological properties of nanoparticle additive and intercalated clay hybrid bentonite drilling fluids. *Journal of Petroleum Science and Engineering.* 2015;127:338-346.

59. Müllen K. Encyclopedia of Polymeric Nanomaterials. Berlin. 2015.